Wind loads on roofs in regions of flow separation

J. D. Ginger and C. W. Letchford

Department of Civil Engineering, The University of Queensland, 4072, Australia.

INTRODUCTION

Extremely large fluctuating suction pressures are usually experienced close to edge discontinuities (ie. leading edges, ridge lines) in regions of flow separation, on roofs of low rise buildings which make these regions highly susceptible to wind induced damage in wind storms. Hence the necessity to study the mechanisms responsible for imposing these large pressures.

FLOW MECHANISMS

Properties of the oncoming freestream flow, shape and dimensions of the structure and its orientation to the wind flow will generate characteristic flow mechanisms with separated shear layers over sharp edged planar roofs. Depending on the characteristics of the flow and that of the structure reattachment of the shear layer may take place, forming either a two dimensional (2D) separation bubble or a three dimensional (3D) conical delta wing vortex.

When flow separation takes place the vorticity diffused from the surface is carried away in the form of a free shear layer and then convected by the velocity field. The balance between diffusion and convection of vorticity distinguishes the two flow mechanisms [1]. When the freestream flow is perpendicular to the line of separation a 2D separation bubble forms with intermittent shear layer roll up into discrete vortices which are then convected with the freestream flow [2]. On the other hand when the flow is at an oblique angle and has a significant component of the freestream velocity in the direction of the edge discontinuity, stationary 3D conical delta wing vortices are formed close to the edge as the vorticity diffused from the surface is balanced by the vorticity that is inherently convected in the direction of the vortex.

PRESSURE DISTRIBUTION

Velocity fluctuations in the oncoming freestream flow and the flow mechanisms induced by the structure lead to a spatially and temporally varying surface pressure distribution on the roof. The design wind load for sections of the roof and its fixtures depend on the magnitude and on the degree of correlation of these pressures over the roof section or section supported by the fixture. The pressure acting on a point (or section) i, on the roof surface may be defined,

$$p_i(t) = \bar{p}_i + p_i'(t) \qquad (1)$$

where, $\bar{p}_i$, p_i' - Mean and fluctuating components of pressure

The covariance, $c_{ij}(\tau)$ is then the statistical quantity which provides information both on the magnitudes and dependence of the fluctuating pressure at a point (or section) i, and pressure fluctuations at another point (or section) j, after a time delay τ and is defined as,

$$c_{ij}(\tau) = \overline{p_i'(t) \cdot p_j'(t + \tau)} \qquad (2)$$

where the overbar in Eq. 2 is a time average. The correlation coefficient is,

$$r_{ij}(\tau) = c_{ij}(\tau) / (\sigma_{pi} \cdot \sigma_{pj}) \qquad (3)$$

where σ_p - Standard deviation of fluctuating pressure

The correlation coefficient $r_{ij}(\tau)$ of surface pressures will depend on the scale of the pressure producing eddies and the time taken for the disturbances

to travel between i and j. As the distance between i and j is increased the small scale disturbances become incoherent and $r_{ij}(\tau)$ decreases, and when there is a component of freestream velocity in the direction i-j, a maxima in $r_{ij}(\tau)$ occurs after a time delay τ.

EXPERIMENTAL PROCEDURE

Tests were carried out in the 3 m wide × 2 m high × 12 m long Boundary Layer Wind Tunnel at the Department of Civil Engineering, University of Queensland. Wind velocity and pressure measurements were carried out using a PC controlled Data Acquisition System. A terrain category 3 (AS-1170) (z_0= 0.2 m) [3] flow, at a length scale of ~ 1/100, and a uniform, low turbulence ($\sigma_U/\bar{U}$ ~ 0.04) flow were simulated in the wind tunnel. A 300 mm × 300 mm, 100 mm high (h) rigid flat roof enclosed building model with a distribution of pressure tappings (closely spaced near the edges) was tested in these flows. The 0° wind orientation was with the flow perpendicular to one edge line. The effect of wind orientation (β), was studied by rotating the model relative to the flow.

Pressure measurements were carried out using tube restrictor systems leading from pressure tappings via Scanivalve switches to Honeywell 163PC pressure transducers fixed under the wind tunnel floor. The pressure measurement systems had good response characteristics up to 100 Hz. The pressures are defined positive in the downward direction, and were lowpass filtered at 100 Hz and sampled at 250 Hz for 60 s.

The mean, standard deviation, maximum and minimum pressure coefficients are defined as,

$$C_{\bar{p}} = \frac{\bar{p} - p_0}{1/2\ \rho\ \bar{U}_h^2}, \qquad C_{\sigma_p} = \frac{\sigma_p}{1/2\ \rho\ \bar{U}_h^2},$$

$$C_{\hat{p}} = \frac{\hat{p} - p_0}{1/2\ \rho\ \bar{U}_h^2}, \qquad C_{\check{p}} = \frac{\check{p} - p_0}{1/2\ \rho\ \bar{U}_h^2}$$

where,

$\bar{p}$, σ_p, $\hat{p}$, $\check{p}$ - Mean, standard deviation, maximum and minimum pressures

p_0 - Reference free stream static pressure

$\bar{U}_h$ - Mean wind speed at roof height, h in freestream flow

ρ - Density of air

Point pressure measurements on the roof model were obtained at β = 0°, 15°, 30° and 45° in both terrain category 3 turbulent boundary layer and uniform low turbulence flows. Corresponding flow visualization tests were carried out using surface oil patterns. Correlation between point pressures close to the leading edges along the line of largest pressures were also obtained.

RESULTS AND CONCLUSIONS

Surface oil flow patterns clearly identify regions of flow separation at the leading edges and the reattachment lines inboard. They also show that an increase in the level of turbulence in the freestream flow reduces the spatial extent of the separation region. The contour plots of mean pressure coefficients obtained from the point pressure study at the worst orientation of 30° in terrain category 3 flow and uniform low turbulence flow are shown in Figures 1 and 2. Maximum, minimum and standard deviation pressure coefficient contour

plots follow the same pattern with C_{σ_p} and $C_{\bar{p}}$ values of large magnitude experienced close to the leading edges. Although standard deviation and peak pressure coefficients of greater magnitude were measured in the higher turbulent boundary layer flow, $C_{\bar{p}}$ s of larger magnitude were obtained in the lower turbulence flow similar to Stathopoulous' [4] results.

The correlation coefficient $r_{ij}(\tau)$, of point pressures relative to tapping A (= h/4, h/20 from leading corner) along the line of large suction pressures x_I, in terrain category 3 boundary layer flow is shown in Figures 3 to 5. These identify the inherent convection of vorticity, with the time delay to maximum $r_{ij}(\tau)$ increasing as the component of freestream velocity in x_I direction increases (ie. as β increases). For $\beta = 0°$, $r_{ij}(\tau)$ of point pressures relative to tapping B (= 3h/2, h/10 from the leading corner) along the line of large suction pressures x_{II} is shown in Figure 6. The spatial correlation $r_{ij}(0)$ under the separation bubble at $\beta = 0°$ and delta wing vortex at $\beta = 30°$, in Figures 7 and 8, show that the pressures are spatially better correlated under the conical vortex than the separation bubble. It is believed that this is due to the stability of the conical vortex flow. Also the conditional correlation coefficient $r^*_{ij}(0)$ indicate that fluctuating pressures ($\geq 2.5 \cdot C_{\sigma_p}$) are better correlated than the background fluctuations.

REFERENCES

1) M. Lee and Chih-Ming Ho, Lift force of delta wings, ASME Applied Mech. Rev.,Vol. 9, (1990) 209-221.

2) P. J. Saathoff and W. H. Melbourne, The generation of peak pressures in separated/reattaching flows, J. Wind Eng. Ind. Aerodyn.,32 (1989) 121-134.

3) Australian standard, SAA loading code Part 2: Wind loads AS 1170.2 - (1989).

4) T. Stathopoulos, Wind pressure loads on flat roofs, BLWT, Research report Fac.of Eng. Sc., The Uni. of Western Ontario, Canada (1975).

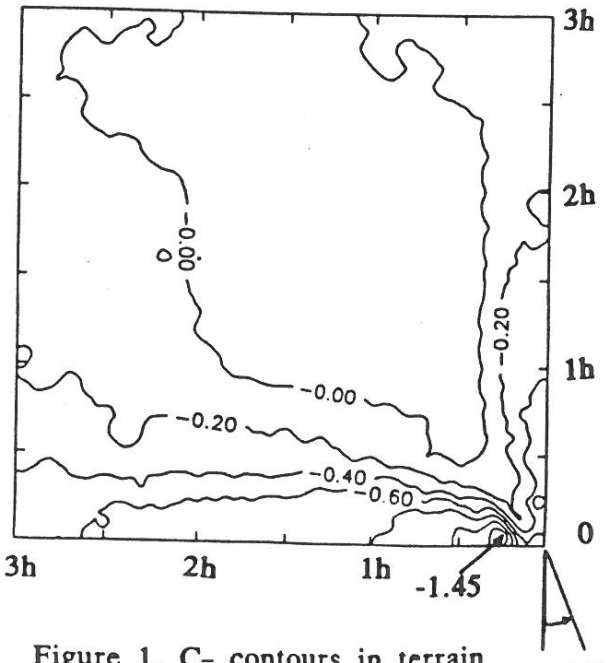

Figure 1. $C_{\bar{p}}$ contours in terrain category 3 flow, $\beta = 30°$.

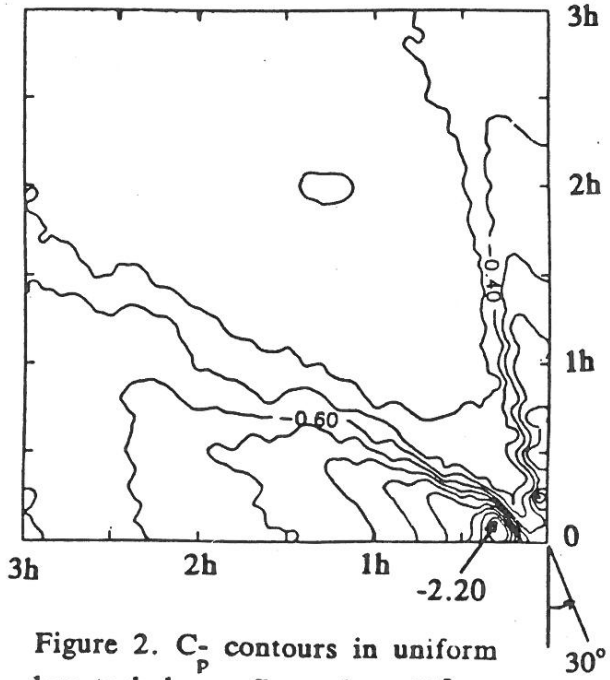

Figure 2. $C_{\bar{p}}$ contours in uniform low turbulence flow, $\beta = 30°$.

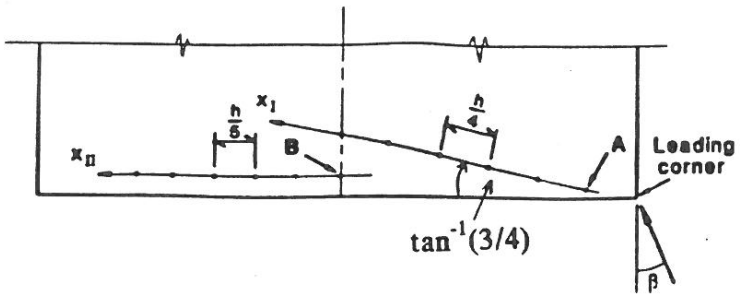

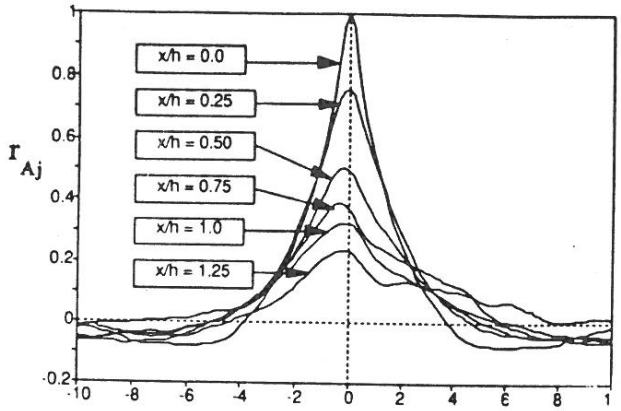

Figure 3. $r_{ij}(\tau)$ relative to A, τ U/h along x_I, $\beta = 15°$.

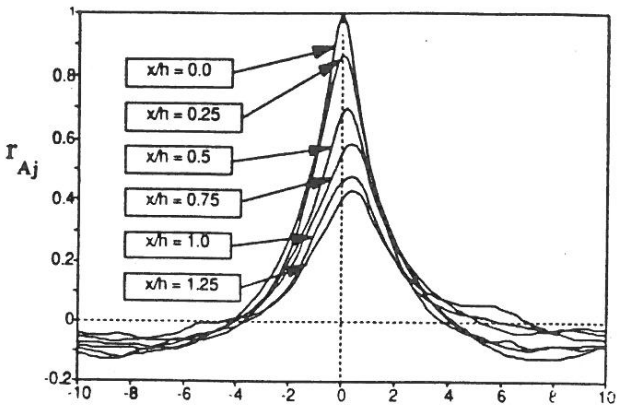

Figure 4. $r_{ij}(\tau)$ relative to A, τ U/h along x_I, $\beta = 45°$.

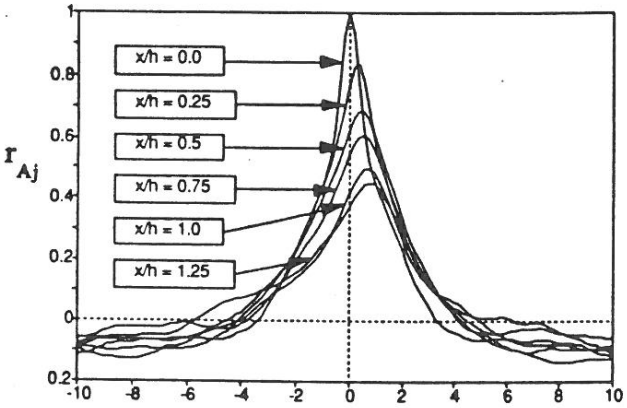

Figure 5. $r_{ij}(\tau)$ relative to A, τ U/h along x_I, $\beta = 75°$.

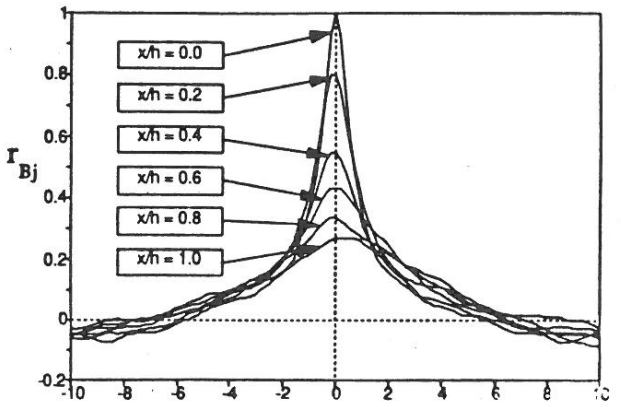

Figure 6. $r_{ij}(\tau)$ relative to B, τ U/h along x_{II}, $\beta = 0°$.

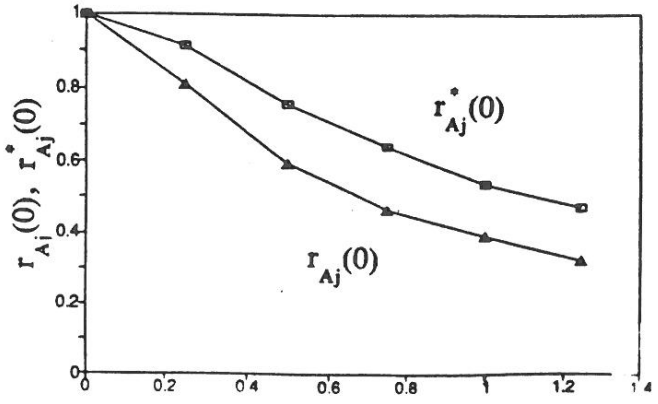

Figure 7. $r_{ij}(0)$ and $r^*_{ij}(0)$ relative to A along x_I, $\beta = 30°$.

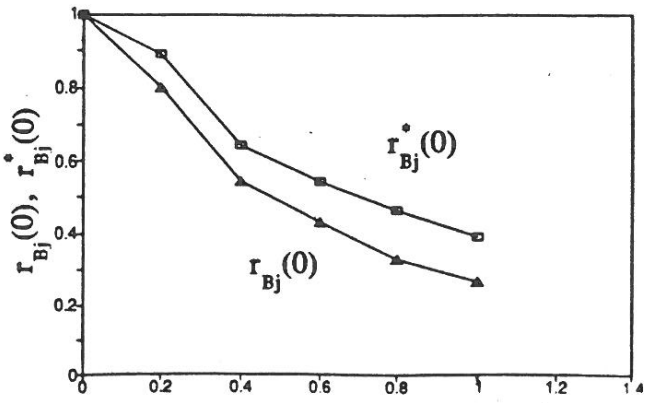

Figure 8. $r_{ij}(0)$ and $r^*_{ij}(0)$ relative to B along x_{II}, $\beta = 0°$.